Pergamon

Int. J. Heat Mass Transfer. Vol. 38, No. 9, pp. 1605–1617, 1995

0017-9310/95 $9.50 + 0.00

0017-9310(94)00287-8

Condensation in a gas-loaded thermosyphon

X. ZHOU and R. E. COLLINS†

School of Physics, University of Sydney, Sydney, NSW 2006, Australia

(*Received* 13 *December* 1993 *and in final form* 18 *August* 1994)

Abstract—An experimental and modelling study is reported of condensation in a cylindrical, two-phase reflux thermosyphon containing non-condensable gas. The diffusion equations in the interface region are solved numerically. The spatial distribution of condensing heat flux is determined from accurate measurements of the thickness of the condensed liquid film. At high power levels, fluctuations can occur in the interface region indicating that, under such conditions, the vapour–gas interface is intrinsically unstable. At lower power levels, stable operation is observed and the width of the interface region is measured as significantly greater than that predicted by the diffusion model. The mass transfer in the interface region is strongly influenced by convection in this domain. At very low power levels, the experimental measurements of spatial distribution of heat flux in the interface region are in excellent agreement with the predictions of the diffusion model, indicating that diffusion is the dominant process which influences condensation in the interface region under these conditions.

1. INTRODUCTION

A two-phase closed reflux thermosyphon is a gravity-assisted wickless heat pipe, consisting of an inclined evacuated tube containing a small quantity of liquid. Vapour, which is generated by heating the working liquid, flows upwards and condenses. The latent heat of the condensation process is transferred through the condenser wall and out of the thermosyphon. The condensate returns to the evaporator under the influence of gravity. Such a device can transport heat over a considerable distance with an extremely small temperature difference.

In addition to the vapour generated from the working liquid, a thermosyphon (or heat pipe) may contain a quantity of non-condensable gas. Such gas may come from microleaks in the walls of the device, dissolved gas in the working fluid, outgassing of internal surfaces of the system, or chemical reactions between the working fluid and the heat pipe wall. Gas may also be deliberately included in the pipe in order to achieve particular heat transfer characteristics. During operation, the non-condensable gas is swept along with the vapour flow and, since it does not condense, accumulates at the end of the condenser. The presence of this gas can significantly change the nature of the transport processes in the condenser. For example, non-condensable gas may completely fill the condenser, effectively inhibiting the operation of the heat pipe. The presence of non-condensable gas can also be utilized to control the range of operating temperatures of the system. In many applications, this is a particularly attractive possibility since the variation in condenser area occurs passively by means of temperature-dependent changes of the gas volume in the condenser. The aim of the present research is to investigate the physical processes which affect condensation in a gas-loaded thermosyphon.

† Author to whom correspondence should be addressed.

2. PREVIOUS WORK

In this section, we briefly review some of the previous theoretical and experimental work on condensation in gas-loaded thermosyphons. The simplest theoretical approach to the analysis of condensation in a gas-loaded thermosyphon (or heat pipe) involves the assumption of a sharp interface between the gas and the condensing vapour. This model was discussed by Marcus [1] and Chi [2]. Initially, axial conduction, diffusion and convection of vapour into the gas plug at the end of the condenser were ignored. In order to improve this model, Edwards and Marcus [3] included one-dimensional (axial) diffusion in the gas–vapour mixture, and axial heat conduction in the condenser wall. A two-dimensional model of a cylindrical system of this type was developed by Rohani and Tien [4]. The elliptical mass, momentum, energy and species conservation equations were solved in conjunction with the overall energy and mass conservation constraints, under steady-state conditions. The results show that energy and mass transfer between vapour and gas may indeed play a dominant role in determining the system performance. However, the results obtained by this model are, to some extent, predetermined by the assumption that the radial temperature variations at the interface between the vapour and the non-condensable gas are parabolic, and that the velocity of vapour at the interface is uniform. Building on the one-dimensional diffuse-front approximation [1, 3], Tien and co-workers [5, 6] developed a two-dimensional model for a cylindrically

NOMENCLATURE

D	diffusivity of gas–vapour mixture
E	dimensionless parameter
F	logarithm of mass fraction of gas
g	acceleration due to gravity
h	heat transfer coefficient
k	Boltzmann's constant
m	molecular mass
p	pressure
R	internal radius of condenser
r	radial co-ordinate
T	temperature
V	velocity of vapour
z	vertical co-ordinate.

Greek symbols

α	heat transfer coefficient to cooling liquid
γ	latent heat of condensation
δ	thickness of layer
θ	dimensionless temperature
κ	thermal conductivity
μ	viscosity
ρ	density of vapour or gas
σ	cross-section for molecular collisions
χ	mass fraction of gas in vapour.

Subscripts

c	cooling liquid
e	empirically determined quantity
f	condensed liquid film
g	gas
i	internal
o	point far below interface
s	saturated
w	wall of condenser.

Superscript

*	dimensionless.

symmetric system which included effects on vapour condensation of both radial and axial mass diffusion of gas. The results of this work demonstrated the inadequacy of the previous, one-dimensional approach which considered only axial diffusion of gas.

Several researchers [7–9] have considered the influence of convective flow on the behaviour of the gas loaded condenser. Such a process results in a great increase in complexity compared with the case where only diffusion is included. The theoretical models in which convective effects are included are all two-dimensional, with Cartesian coordinates, and involve significant simplifying assumptions.

There has been extensive experimental work on the performance of gas-loaded heat pipes and thermosyphons. In general, measurements of overall heat transfer rates do not provide much detail about the physical processes which determine the performance of these systems. Recently, a few studies have provided more detailed information about the gas-loaded system by using new experimental techniques. Galaktionov and Trukhanova [8] used a laser Doppler anemometer to confirm the existence of reverse flow phenomena in a horizontal heat pipe. Parfentiyev [10] measured the temperature gradient within the vapour near a wicked condenser surface and obtained the local heat flux under the assumption that the vapour in this region is saturated. This work showed that the shape of the interface is influenced by the bulk vapour flow. Peterson and Tien [11] used a wet-bulb/dry-bulb method to measure the vapour concentration distribution around the gas–vapour interface. Measurements showed that the vapour in the gas is not saturated, and that natural convection has a large influence on the interface. The agreement between the experimental results and theoretical work [5, 6] is not particularly good, however. Kobayashi and Matsumoto [12] used a laser holographic interferometer to obtain temperature and density information, and the mole fraction of non-condensable gas, in the interfacial region of a planar condensation system. The results showed that the flow field in the vapour–gas mixing region is characterized by a well-defined interfacial layer. Zhou and Collins [13–15] developed a novel, rotating needle contact method, for studying the condensation in a thermosyphon. The distribution of heat and mass transfer rate in the condenser was determined by measuring the thickness of the condensed liquid film. This method differs from that used by Reed and Tien [16], who measured the spatial distribution of condensing heat flux in a system without non-condensable gas using several heat flux meters on the external surface of the condenser.

In most of the above studies, instabilities near the vapour–gas interface, as evidenced by temperature fluctuations, were commonly observed in gas-loaded thermosyphons or heat pipes. Such instabilities were attributed to bursts of strong boiling in the evaporator [12] and to natural convection effects in the interface [11].

In the present work, we study transport phenomena in condensers of thermosyphons with particular emphasis on gas-loaded condensers. The temperature distribution in the condenser, and the thickness of the condensed liquid film, are measured. These results are used to determine the spatial distribution of heat flux in gas-loaded condensers. In addition, the transport processes in this system are modelled using numerical techniques, on the assumption that the dominant transfer process in the interface region is diffusion. Particular attention is given in the numerical analysis to the development of a method of specifying the

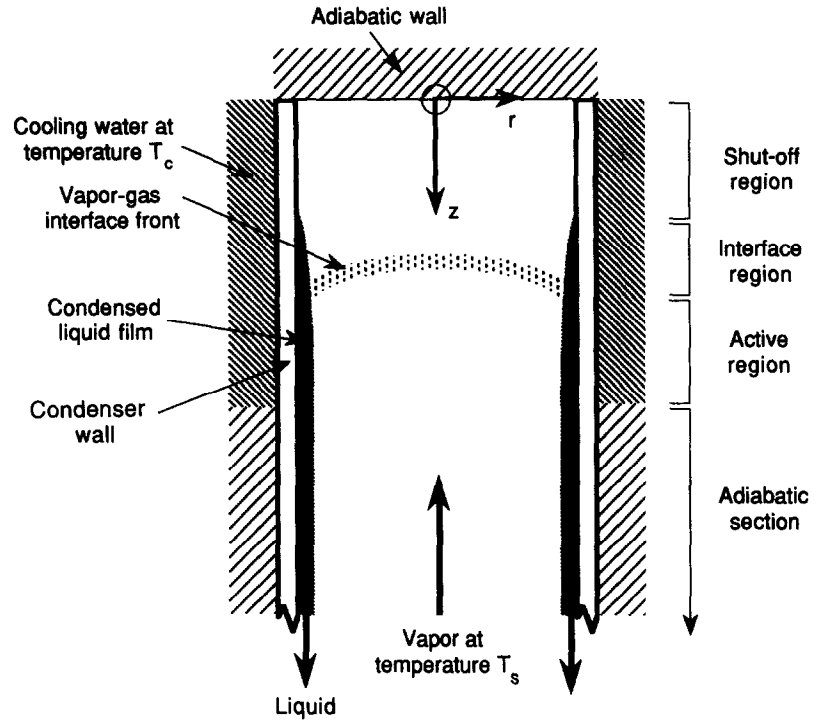

Fig. 1. Schematic diagram of the system for studying condensation in the presence of non-condensable gas.

boundary conditions in a way that does not affect the results of the calculation but which retains the essential physical features of the process. The approach taken permits more rapid calculation than other methods and makes it possible to extend the analysis to extremely small values of gas mole fraction.

3. THEORETICAL ANALYSIS OF A GAS-LOADED THERMOSYPHON

In a gas-loaded thermosyphon, the gas molecules experience collisions with molecules of the condensing vapour as the vapour is transported along the thermosyphon. The directed momentum of the vapour tends to concentrate the non-condensable gas at the condenser end of the thermosyphon. The non-condensable gas can therefore inhibit the free motion of the vapour to the surface of the condenser. A cylindrical condenser (Fig. 1) is characterized by three distinct regions in which the condensation processes are qualitatively different. At the bottom of the condenser, the concentration of non-condensable gas is negligible, and pure vapour condensation occurs. This is called the active region. The temperature in this region is quite uniform, and higher than that of the external cooling fluid by an amount dependent on the heat flow associated with the condensing vapour. At the top of the condenser, a region exists which contains an essentially stagnant mixture of gas and vapour. Negligible heat transfer occurs in this part of the condenser, which we call the shut-off region. The temperature in this region is also nearly constant, and is very close to that of the external cooling fluid. Between the upper and lower regions, a gas–vapour interface region exists in which there is a mixture of condensing vapour and non-condensable gas. The transport phenomena in this region may include mass diffusion, conduction, convection and radiation. The study of this region is central to the present work.

Zhou [15] has shown that the two processes which can make significant contributions to the motion of vapour in the interface region are thermal diffusion and convection. In the theoretical analysis presented here, we consider only diffusion. We subsequently present experimental data at low power levels which are in extremely good agreement with the results from this model. At higher power levels, however, the modelling and experimental results are not in good agreement, from which we will infer that convective processes are indeed important in such cases.

Our analysis initially follows that of Hijikata *et al.* [6]. We consider steady-state transport by diffusion of the condensable vapour through the stationary non-condensable gas in the cylindrically symmetric condenser illustrated in Fig. 1. Since temperature differences in the system space are quite small, the density of the gas–vapour mixture is assumed to be constant, and equal to the saturated density of the incident vapor, ρ_s. Hijikata *et al.* apply Fick's diffusion law to this system and show that the mixture velocity **V** can be written:

$$\mathbf{V} = D\nabla(\ln \chi_g) \tag{1}$$

where D is the diffusivity, and

$$\chi_g = \rho_g/\rho_s \tag{2}$$

is the mass fraction of the gas.

Application of the continuity equation gives:

$$\nabla^2(\ln \chi_g) = 0 \tag{3}$$

where the diffusivity is taken to be constant.

We adopt the following boundary conditions:

$$\text{At} \quad z = 0 \quad V_z = 0 \quad \text{or} \quad \partial(\ln \chi_g)/\partial z = 0 \tag{4}$$

$$\text{at} \quad z = z_o \quad \chi_g = \chi_g(z_o) \tag{5}$$

$$\text{at} \quad r = 0 \quad V_r = 0 \quad \text{or} \quad \partial(\ln \chi_g)/\partial r = 0 \tag{6}$$

$$\text{at} \quad r = R \quad \rho_s D(\partial \ln \chi_g)/\partial r = h_c(z)(T_i(z) - T_c)/\gamma. \tag{7}$$

The first and third boundary conditions, equations (4) and (6), respectively state that no condensation occurs on the end wall of the condenser, and that the system is cylindrically symmetric. These boundary conditions were also used by Hijikata *et al.* The second boundary condition, equation (5), requires the choice of a very small value for the gas mole fraction $\chi_g(z_o)$, at a point, z_o, far below the interface. Typically, z_o is ~ 10 diameters below the interface and $\chi_g(z_o)$ is $\sim 10^{-100}$. This approach removes the necessity to assume a particular functional form for the solution close to the interface, as was done by Hijkata *et al.* The values of $\chi_g(z_o)$ and z_o are varied by trial-and-error to locate the interface at the desired position in the condenser, and thus to determine the total amount of non-condensable gas in the system.

The fourth boundary condition, equation (7), arises from the transfer of heat from the condensing vapour to the external cooling fluid. Hijikata *et al.* assumed that the condensed liquid film is sufficiently thin that this heat flow can be characterized by a constant heat transfer coefficient. This assumption is appropriate when thermal impedances from other sources limit heat flow. Such impedances may, for example, be due to a relatively insulating condenser wall, such as glass, or to the heat transfer from the outer wall of the condenser to the cooling fluid. We are also interested in the situation, which is of some practical importance, where the heat transfer may be dominated by the impedance of the condensed liquid film itself. In equation (7), $T_i(z)$ and T_c are the temperatures just inside the condenser and in the cooling fluid, respectively, and γ is the latent heat of condensation of the vapour. This boundary condition differs from that of Hijikata *et al.* in that the heat transfer coefficient from the inner surface of the condensed liquid film to the cooling fluid, $h_c(z)$, is dependent on the thickness of the liquid film and therefore on position in the condenser. We write:

$$h_c(z) = [\delta_f(z)/\kappa_f + \delta_w/\kappa_w + 1/\alpha_c]^{-1} \tag{8}$$

as the combination of the heat transfer coefficients for heat flow through the condensed liquid film ($\kappa_f/\delta_f(z)$), through the condenser wall (κ_w/δ_w), and from the outer surface of the condenser to the cooling liquid (α_c). The thickness of the condensed liquid film is calculable through the Nusselt solution for the falling film:

$$(g\rho_f^2 \delta_f^2(z)/\mu_f)\, \mathrm{d}\delta_f/\mathrm{d}z = \rho_s D[\partial(\ln \chi_g)/\partial r]_{r=R} \tag{9}$$

which can be re-written as an integral relation over the part of the condenser from 0 to z. Clearly this boundary condition, equation (7), implicitly includes the solution to the equations, and a self-consistent method must be used to obtain that solution, as discussed below.

In addition to the above four boundary conditions, equations (4)–(7), it is necessary to relate the two system variables—the mass fraction of the gas, χ_g, and the temperature in the system T_i. Again, following Hijikata *et al.* [6], this is done by assuming that the gas–vapour mixture is saturated adjacent to the condensed liquid film. We use the same relationship, derived from the Clausius–Clapeyron equation, that was adopted by Hijikata *et al.* between the vapour pressure and temperature at the film, and write:

$$\text{at} \quad r = R: \quad \chi_g = 1 - (T_s/T_i)\exp[T_e(1 - T_s/T_i)] \tag{10}$$

where T_e is a dimensionless temperature and is chosen to give values in agreement with experimental vapour pressure data.

It is convenient to introduce dimensionless variables:

$$r^* = r/R \quad z^* = z/R \tag{11}$$

$$\theta = (T_i - T_c)/(T_s - T_c) \quad \theta_c = T_c/(T_s - T_c). \tag{12}$$

The differential equation (3) can now be written:

$$\frac{\partial^2 F}{\partial r^{*2}} + \frac{1}{r^*}\frac{\partial F}{\partial r^*} + \frac{\partial^2 F}{\partial z^{*2}} = 0 \tag{13}$$

where

$$F = \ln \chi_g \tag{14}$$

with the boundary conditions

$$\text{at} \quad z^* = 0 \quad \partial F/\partial z^* = 0 \tag{15}$$

$$\text{at} \quad z^* = z_o/R \quad F = \ln \chi_o \tag{16}$$

$$\text{at} \quad r^* = 0 \quad \partial F/\partial r^* = 0 \tag{17}$$

$$\text{at} \quad r^* = 1 \quad \partial F(z)/\partial r^* = 0/E(z) \tag{18}$$

where

$$E(z) = \rho_s D\gamma/h(z)(T_s - T_c)R \tag{19}$$

and $h(z)$ is given by equations (8) and (9). Once again we note that, in cases where the heat transfer is significantly influenced by the condensed liquid film, the fourth boundary condition, equation (18), implicitly involves the solution, and self-consistent methods must be used to satisfy it. In addition to these boundary conditions, we have a relation derived from equation (10):

$$F = \ln\left\{1-\left(\frac{1+\theta_c}{\theta+\theta_c}\right)\exp\left[T_c\left(\frac{\theta-1}{\theta+\theta_c}\right)\right]\right\}. \quad (20)$$

Equation (13) can also be used to calculate the gas concentration in the adiabatic region below the condenser. In this case the boundary condition, equation (18), is simply replaced by:

$$\text{at} \quad r^* = 1 \quad \partial F(z)/\partial r^* = 0 \quad (21)$$

corresponding to zero condensation in this region.

The solution of these equations is performed numerically using conventional difference techniques. A difficulty arises for points in the condenser far below the interface when the gas mass fraction χ_g is very small. In this region, the temperature in the condenser, T_i, is very nearly equal to the temperature of the incoming vapour, T_s, and the reduced temperature θ is very close to unity. Direct application of the difference equations under such conditions can give rise to large round-off errors, and consequent instabilities in the solution. It is even possible for the argument of the logarithm in equation (14) to become negative, and the iteration process breaks down. This problem can be simply avoided by recognizing that the lack of variability of θ in this region enables a solution for F to be written at the wall of the condenser ($r^* = 1$) by inspection from the boundary condition, equation (18):

$$\partial F/\partial r^* = \theta/E. \quad (22)$$

By treating θ as a constant, the solution for F can be written directly from this equation and, by substitution into the main differential equation (13), we can derive the full dependence of F on r and z. Operationally, this procedure is implemented by requiring that, whenever the iteration leads to a value of θ which is greater than 0.999, the value of θ is set by default at 0.999. This leads to a negligible error in the gas concentrations, and permits the establishment of a lower boundary condition at a point which is far below the interface where the gas fraction is extremely small, and the temperature is almost constant. The validity of this approach is demonstrated by the fact that no discontinuities can be seen in any of the calculated parameters, or in their gradients, in the region where θ assumes its fixed value of 0.999.

As has been noted, the boundary condition, equation (18), requires a self-consistent approach to the calculation in cases where the thermal impedance of the liquid film significantly influences the heat flow from the condensing vapour to the cooling water. In order to solve this problem, an approximate distribution is assumed for the thickness of the condensed liquid film and the diffusion equation is solved with this distribution in the boundary conditions, equations (18) and (19). The solution so obtained is used to calculate a new distribution for the thickness of the film, and the process is repeated until the results change by less than a small, specified amount.

Obviously, in situations where the liquid film does not significantly affect the heat transfer to the cooling fluid, such as in a glass-walled condenser, this procedure is unnecessary. In such cases, the heat transfer coefficient in equation (19) can be assumed to be independent of position.

It is important at this stage to consider the dependence of the results of the diffusion model on the quantities in the governing equations and boundary conditions. It is clear from the dimensionless form of equations (13)–(19) that the parameter which controls the width of the interface is E, in equation (19). The value of E determines two important features of the solution. Firstly, the rate of decrease of the concentration of non-condensable gas below the interface is a very strong function of E; larger values of E result in a much more rapid decrease in concentration. This can be seen directly from equations (13) and (18) by setting $\theta \simeq 1$ for regions below the interface. Secondly, the value of E affects the width of the interface region itself. E is of the same order as the ratio of the heat flux per unit area through the interface to that through the condenser wall. An increase in E would therefore be expected to increase the width of the interface, and a series of modelling calculations shows that this is indeed the case. However, it turns out that the width of the interface region depends only weakly on the value of E. For example, it is found that a 30% increase in the value of E from 1.12 to 1.45 results in only 20% change in the width of the interface, from 3.0 to 3.6 condenser radii (where the width is measured between the 10 and 90% values of temperature difference across the interface).

On the basis of this discussion, we would expect to find variations of the width of the interface, albeit relatively small ones, with changes in the factors that determine the parameter E. The three factors to be considered are ρ_s, D and $(T_s - T_c)$. It is well known [17] that, for self-diffusion, the product of gas density ρ and diffusion constant D is:

$$\rho D = 2(kTm)^{1/2}/3\pi^{3/2}\sigma^2 \quad (23)$$

where m is the molecular mass and σ is the cross-section for molecule–molecule collisions. Equation (23) can be re-written in an alternative convenient form:

$$pD = 2(kT)^{3/2}/3m^{1/2}\pi^{3/2}\sigma^2 \quad (24)$$

where p is the pressure in the system.

The situation for gas mixtures is more complex, but collision integral approaches give a result, which is well validated experimentally, that has the same functional dependencies as in equations (23) and (24) with the molecular mass m replaced by the reduced mass $m_1m_2/(m_1+m_2)$ of the two gas species [17].

For our numerical modelling, we use an empirical form [18] for the diffusion constant for air and water vapour:

$$D = 9.86 \times 10^{-5} T^{1.81}/p \, [\text{m}^2\,\text{s}^{-1}]. \quad (25)$$

On the basis of these relationships, we can conclude that, for given types of condensable vapour and non-condensable gas, the major variations in the parameter E should arise from changes in the temperature difference across the interface. The diffusion model predicts, for example, that the width of the interface should decrease as the input power to the condenser increases for constant gas load. In the following, we show that, under certain experimental conditions (specifically at very low input power), this is indeed observed. At higher power levels, however, we will show that departures from this behaviour occur, from which we conclude that physical processes other than diffusion are important in such cases.

4. EXPERIMENTAL APPARATUS AND DATA ANALYSIS

The aim of the experiment is to characterize the behaviour of the condensation process in the interface region of a gas-loaded thermosyphon in sufficient detail that the physical mechanisms which govern that process can be determined. The experimental apparatus was therefore designed to measure the spatial dependence of condensing vapour and the temperature in the vicinity of this interface.

A schematic diagram of the experimental apparatus is shown in Fig. 2. The design and operating principles of the apparatus are described in an earlier paper by Zhou and Collins [14]. Briefly, vapour from a heated source is directed into a water-cooled, cylindrical condenser. The condensed liquid flows back to the vapour source chamber under gravity. The rate of flow of this liquid can be measured using a calibrated volume in the return line. The system can be evacuated externally, and controlled amounts of gas can be admitted. The axis of the condenser can be inclined at any desired angle to the vertical.

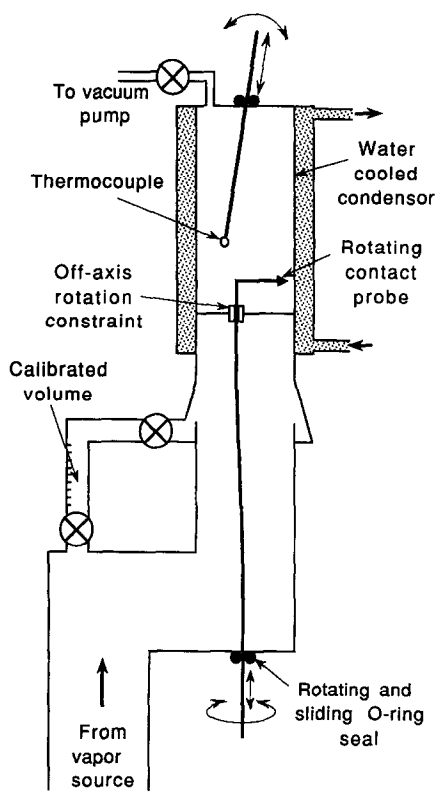

Fig. 2. Schematic diagram of experimental apparatus.

Accurate measurements are made of the spatial dependence of the thickness of the condensed liquid film using a contact probe. The position of the probe relative to the wall of the condenser can be controlled to high accuracy by rotating it about an axis which is parallel to the axis of the condenser, but displaced slightly from it. The thickness of the condensed liquid film is determined by detecting the points of contact of the probe with the free surface of the film, and with the wall of the condenser. For films which are sufficiently thin that the surface is free of waves [19], the thickness of this film can be related to the distribution of condensing vapour through the Nusselt solution [20] for a falling film, equation (9). Zhou and Collins [14] describe the application of this method to condensers with electrically insulating walls, such as glass, and with electrically conducting walls, such as copper. They also detail the techniques used to achieve appropriate experimental conditions, including uniform wetting of the surface of the condenser, a steady source of vapour, and stable operation over long periods of time. The methods used to obtain the spatial dependence of condensing vapour from the experimental film thickness data are also described.

Zhou and Collins [14] present experimental results which validate this technique. Measurements are reported in a glass-walled condenser with no non-condensable gas, for which the spatial dependence of condensing vapour, and therefore of thickness of liquid film, are calculable. Preliminary data are also given of the condensing heat flux in a glass walled condenser containing non-condensable gas. In such a condenser, the glass wall represents the dominant thermal impedance for heat flow from the point of condensation to the cooling fluid. The spatial dependence of heat flux in this system can therefore also be determined from measurements of the temperature difference between the condensed liquid film and the cooling fluid. The results of the two methods for estimating the spatial dependence of heat flux are shown to be in excellent agreement.

We have further validated the experimental method by determining the spatial dependence of condensing heat flux in a copper condenser without non-condensable gas. In this situation, the dominant thermal impedance for heat flow between the point of condensation and the cooling fluid is that of the liquid film itself, although the heat transfer from the outer wall of the condenser to the cooling fluid also has a small effect. The spatial distribution of condensing vapor in this situation, derived from the measurements of film thickness, is found to agree well with

that calculated on the basis of the above two heat transfer mechanisms. The best fit between experimental data and calculated film thickness is obtained for a heat transfer coefficient for heat flow from the outer wall of the condenser to the cooling liquid of 9600 W m^{-2} K^{-1}. This is in close agreement with the value which is calculated from the flow rate of the cooling liquid in the condenser.

We believe that this result and the data presented in the earlier paper [14] provide strong validation of the usefulness of this method for studying the details of the condensation process in gas-loaded thermosyphons.

5. RESULTS

In this section, we report on measurements of condensation in the presence of non-condensable gas in both glass and copper cylindrical condensers. The important features of the condensers used in the present work, and the physical constants of materials in the liquid film and condenser walls, are shown in Table 1. Water is used as the working fluid. The thickness of liquid film given in Table 1 is that at the bottom of the condenser under typical experimental conditions, and is calculated from an integration of equation (9). It is clear that in a glass-walled condenser, the total thermal impedance between the vapour and the cooling water is dominated by the glass wall. Therefore, the condition of uniform condensation in the pure vapour region within this condenser is satisfied very well. In contrast, in a copper-walled condenser, the impedance for heat flow varies with the thickness of liquid film.

The heat and mass transfer in the vicinity of the gas–vapor interface are influenced by many factors, including the physical properties of the working material, the inside and outside temperatures of the system, the input power, the amount of gas and the gas species, and the orientation and geometry of the thermosyphon. In the present work, we present results of the interface shape, interface width and the heat flux distributions in the interface. These results lead to an identification of the dominant physical processes which influence the condensation process in the vicinity of the interface.

Time-dependent effects

We first consider non-steady-state effects. It is found that, in a glass-walled condenser at sufficiently high power levels, the temperature in the vicinity of the vapour–gas interface fluctuates indefinitely. In contrast, in a copper-walled condenser, no fluctuations are observed under any conditions, to the detection limit of the thermocouple (0.1°C).

A series of experiments was conducted to determine the physical mechanisms which lead to the fluctuations in a glass-walled condenser. In the experiments, the temperature is recorded as a function of time within the interface region of the condenser at various power levels. The thermocouple is located close to the axis of the condenser. The condenser is carefully aligned to be co-axial with the adiabatic section. Measurements are made with the thermosyphon positioned vertically, and also inclined to the vertical. The most rapid fluctuations occur over times ~ 1 s, which is approximately equal to the thermal response time of the temperature sensor. Fluctuations are larger at higher power levels (or larger temperature differences across the interface) and the magnitude of the fluctuations increases much more rapidly than either the power level or the temperature difference across the interface. Fluctuations which occur with helium in the condenser are smaller than with air.

It was found that the fluctuations which are observed in the glass condenser of an inclined thermosyphon are basically the same as those occurring in a vertical one. No stratification flow [10] is observed, as was seen by Peterson and Tien [11], and the time-averaged temperature distribution in the vicinity of the interface is still symmetric about the axis. This is a surprising result. If the flow pattern in the interface is dominated by natural convection, we would expect different behaviour in an inclined condenser since natural convection depends on the angle of the system. It is likely, therefore, that forced convection, caused by the bulk vapour flow to the interface, is an important factor in the origin of these fluctuations.

More details of the nature of the fluctuations are obtained by simultaneously recording the temperature at two points within the condenser: one close to the axis of the condenser and the other near the inner surface. It is found that the temperature changes

Table 1. Physical parameters for the condenser

	Condenser wall		Liquid film
	Glass	Copper	Water
Outer diameter [mm]	26.0	25.4	
Inner diameter [mm]	23.0	23.4	
Thickness [mm]	1.5	1.0	0.05
Thermal conductivity [W m^{-1} K^{-1}]	1.0	384	0.56
Thermal impedance [m^2 K W^{-1}]	1.5×10^{-3}	2.6×10^{-6}	1.0×10^{-4}

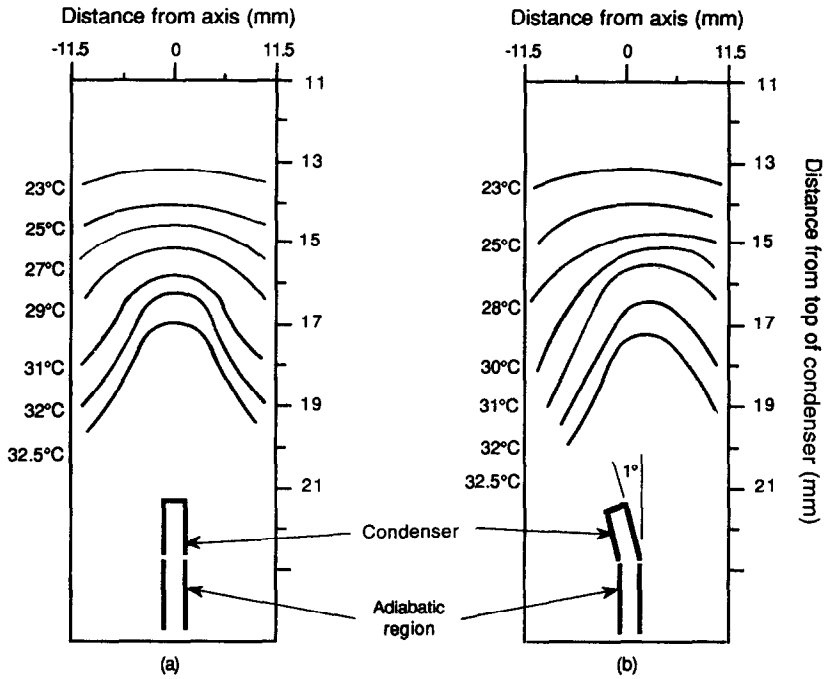

Fig. 3. Temperature profiles within a glass-walled condenser, the axis of which is slightly misaligned with respect to that of the lower adiabatic region. (a) Measurements along a direction which is perpendicular to the plane defined by the axes of the condenser and the adiabatic region; (b) data in this plane. The working fluid is water, with air as the non-condensable gas. The input power is 113 W.

measured by the two thermocouples are in opposite directions: an increase in temperature on the axis of the condenser is accompanied by a decrease near the wall. This observation indicates that the fluctuations are associated with a change in the shape of the interface, rather than a movement along the condenser of the entire interface. The total volume of the non-condensable gas does not appear to change significantly.

Measurements were made on a thermosyphon in which the condenser was deliberately misaligned off the axis of the system by about 1°. This misalignment results in a qualitative change in the shape of the interface, from symmetric in the aligned system, to asymmetric as shown in Fig. 3. We also find that the fluctuations are no longer present, the temperature measured in the vicinity of the interface being constant to the limit of sensitivity of the thermocouple detection system (0.1°C). In comparison, at the same working conditions, temperature fluctuations of ± 1.5°C occur in the aligned system.

These observations provide strong evidence that the fluctuations do not arise from pressure changes in the system due to instabilities in the boiling process. Such changes would simply move the entire interface up and down the condenser and the corresponding temperature variations on the axis and near the wall would be in-phase. In addition, a slight misalignment of the condenser relative to the axis of the thermosyphon would not eliminate the fluctuations if they arose from instabilities in the boiler.

We provide the following tentative explanation for these observations. It appears that the interface between the condensing vapour and the non-condensable gas is only just mechanically stable. Instabilities may be initiated by, for example, a local increase in condensation rate at one point in the interface, which causes a corresponding localized temperature and pressure change at this point and a consequent movement of the non-condensable gas. The power dependence and the difference in behaviour for helium and air appear to imply that natural convection effects in the vicinity of the interface may act as triggers which initiate such instabilities. The absence of fluctuations in the misaligned condenser, and the stable, asymmetric interface that exists for this configuration, lend support to the idea that the symmetric interface is not far from a stability limit.

In the rest of this paper, all the measurements that are discussed are made with aligned condensers at power levels for which fluctuations are absent.

Effect of species of non-condensable gas

We now describe the effect of the species of non-condensable gas in the condenser. Experiments in a glass-walled condenser are discussed, at two power levels (110 and 76 W) with helium and air as the non-condensable gases. The amount of helium was chosen to give the same temperature difference between the pure vapour region and the cooling water at 110 W as

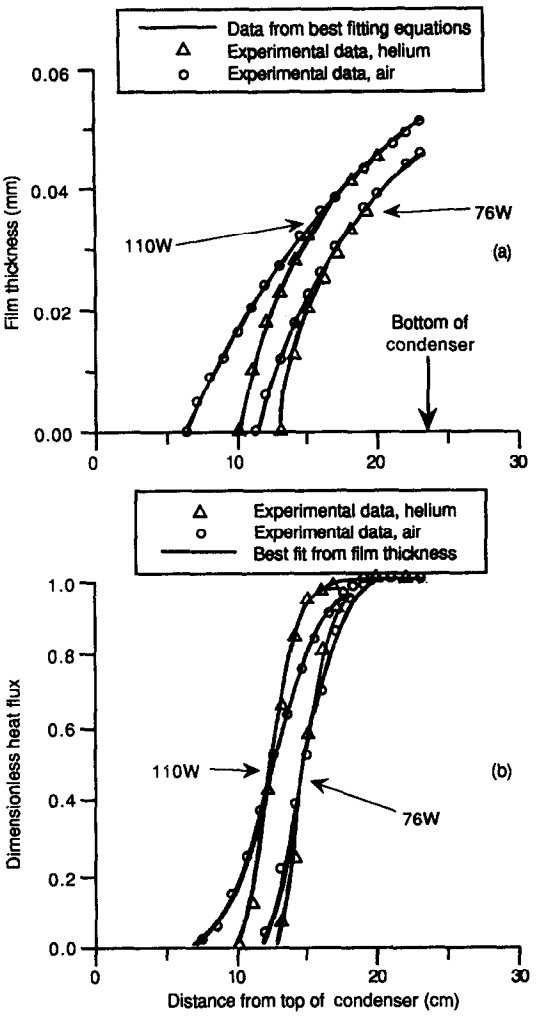

Fig. 4. The data points in (a) show the measured thickness of condensed liquid film in a glass-walled condenser containing air and helium as non-condensable gas and water as the working fluid. These data are used to determine the spatial distribution of condensing vapour shown as lines in (b). The lines in (a) are values of film thickness recalculated from the derived spatial distributions shown in (b). The points in (b) are independent measurements of the heat flux in the glass-walled condenser obtained from data for the temperature difference across the wall.

in the air-filled condenser. The quantities of air and helium were not changed for the measurements at 76 W.

The points in Fig. 4(a) show measurements of thickness of condensed liquid film along the condenser. Values of local heat flux, calculated by curve fitting of the film thickness data, are shown as lines in Fig. 4(b). Data for the spatial distribution of heat flux, independently determined from measurements of temperature difference between the inner liquid film and the coolant, are also shown as data points in Fig. 4(b). The excellent agreement between the results of the two independent methods provides further strong confirmation of the validity of the film thickness technique [13–15]. The self-consistency of the curve-fitting method is illustrated by the values of film thickness [lines in Fig. 4(a)], which are re-calculated from the best fitting curves of heat flux in Fig. 4(b) using methods described in ref. [14].

These results clearly show the three distinct regions in the condenser: active, interface and shut-off. As expected, for the same gas species and quantity, the length of the active region is greater at higher power levels since the system pressure increases with evaporator temperature. More significantly for this work, at higher power levels the width of the interface increases, and a greater proportion of heat transfer occurs in the interface region. This effect is less pronounced for the condenser containing helium. We also note that, under otherwise identical working conditions, the interface width in the air–water system is greater than that in the helium–water case.

As discussed previously, the width of the interface, as calculated from the diffusion model, is expected to be less for larger temperature differences across the interface, and for more massive molecules in the gas–vapour mixture. The experimental results in Fig. 4 are in qualitative disagreement with this model in both cases. These results therefore lead us to conclude that convective effects play an important role in the transfer processes in the vicinity of the interface in these experiments.

Results of measurements of the interface width in a copper condenser with different species of non-condensable gas are consistent with this conclusion. In this case, the interface width, at a given power level, is measured to be approximately the same for both helium and air as non-condensable gas. In addition, the width stays approximately the same as the power level is changed. Convective effects are believed to be still present in the copper condenser, but of lesser magnitude, due to the reduced temperature difference across the interface. It appears that, in the copper condenser, the effects of convection and diffusion on the width of the interface roughly compensate each other.

Effect of working temperature

We next discuss the effect of changing the working temperature below the interface (and therefore the pressure in the system) whilst other conditions in the vicinity of the interface are kept constant. Measurements were made in a glass condenser at three different evaporator temperatures. The amount of non-condensable gas in the condenser and the input power to the boiler were systematically adjusted so that the position of the interface and the temperature difference across the interface were approximately the same in each case. For such conditions, the diffusion model predicts that the width of the interface should be the same in each case, since the factor $\rho_s D$ in the scaling parameter E [equation (19)] is nearly independent of pressure.

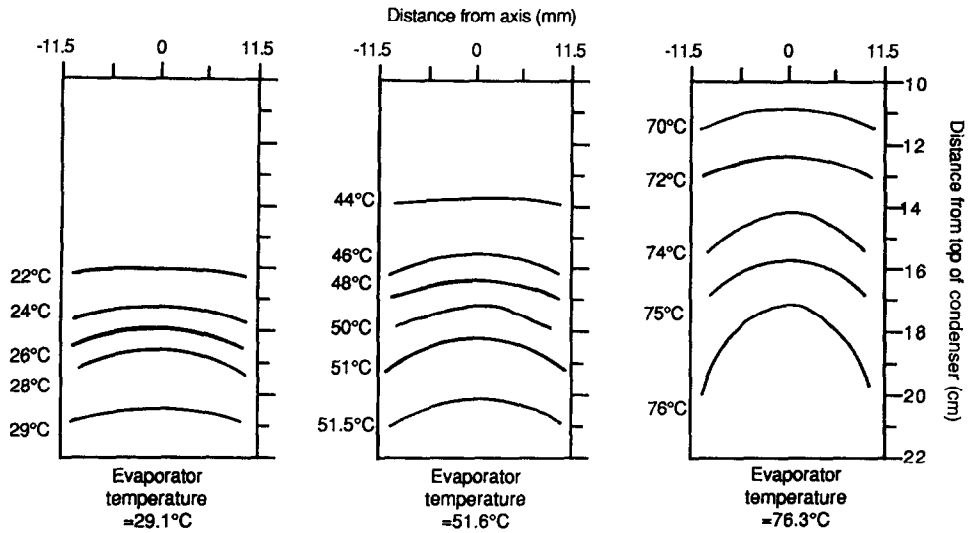

Fig. 5. Isotherms in a glass condenser for different working temperatures with water as working fluid, and air as non-condensable gas. In these measurements, the heat flux below the interface, and the temperature difference across the interface, are both adjusted to be approximately the same for each operating temperature. The broadening of the interface with increasing temperature is clearly evident.

Figure 5 shows the measured isotherms in the vicinity of the interface for the three different working temperatures: 29.1, 51.6 and 76.3°C. Air is used as the non-condensable gas in these experiments. In contrast to the predictions of the diffusion model, the data clearly show that the width of the interface increases with temperature. This disagreement again indicates the existence of significant mass transport in the vicinity of the interface by mechanisms other than diffusion, providing further support for the argument that convective effects contribute significantly to transport in the interface region in these experiments.

Comparison of experimental and modelling results

The previous discussion provides strong evidence of the importance of convective effects in the interface region of condensers containing non-condensable gas. The increases observed in the width of the interface with increasing power levels are not qualitatively consistent with the diffusion model, which predicts that the interface width should decrease under such conditions. In this section, the results of the experiment and the diffusion model are compared quantitatively. It is shown that experimental conditions can be established in which the measured interface parameters are in very close agreement with the predictions of the diffusion model. Under such conditions, convective effects presumably make a negligible contribution, and the transport processes in the vicinity of the interface are determined entirely by diffusion.

Figure 6 compares the results of the diffusion model with experimental measurements for a copper condenser with air as non-condensable gas at a power level which leads to a relatively large heat flux below the interface. Figure 6(a) shows experimental data for the thickness of the condensed liquid film (points) and the film thickness calculated from the diffusion model (line). The experimental results are used to determine the spatial dependence of condensing heat flux in the interface region, as shown in Fig. 6(b). The data of Fig. 6(b) are used to determine the reduced temperature difference between the condensing vapour and the cooling fluid, and Fig. 6(c) compares the reduced temperature difference obtained in this way with the predictions of the diffusion model.

Figure 7 compares experimental and modelling results for dimensionless heat flux (which in this case is equal to dimensionless temperature) for a glass condenser at power levels corresponding to relatively high values of heat flux below the interface.

The data in Figs. 6 and 7 show that the experimentally measured width of the interface is significantly greater than that determined from the diffusion model. As before, we attribute the differences to convective effects in the interface region. In this regard, it is important to recognize that the critical parameter which characterizes the condition of the interface is not the absolute power level in the evaporator, but the temperature difference across the interface. The two quantities are interdependent through the position of the interface which is determined by the amount of non-condensable gas in the thermosyphon.

Figure 8 shows experimental and modelling results for a glass condenser at a power level corresponding to a much reduced temperature difference across the interface (7°C) and a similarly lower heat flux below the interface. The lines in this figure respectively show the modelling results for: (a) the temperature in the

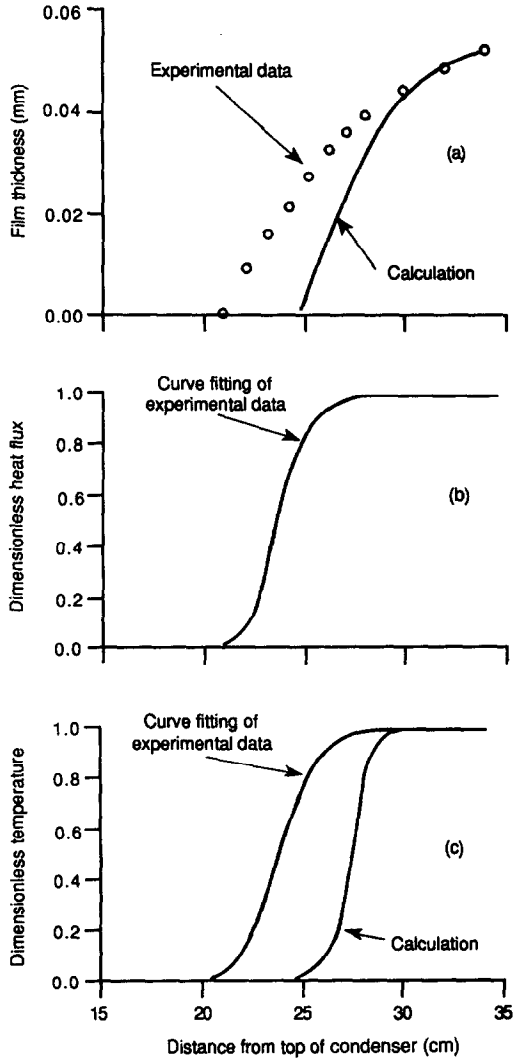

Fig. 6. Comparison of results from the diffusion model with experimental data at a relatively high power level (101 W) in a copper condenser with water as working fluid and air as the non-condensable gas. (a) Experimental measurements of the thickness of the condensed liquid film (points) and the results from the model (line). (b) The dimensionless heat flux, as determined from the experimental measurements in (a). (c) Comparison of experimental and modelling results for the dimensionless temperature in the interface. The experimental data in (c) are calculated from the heat flux data of (b).

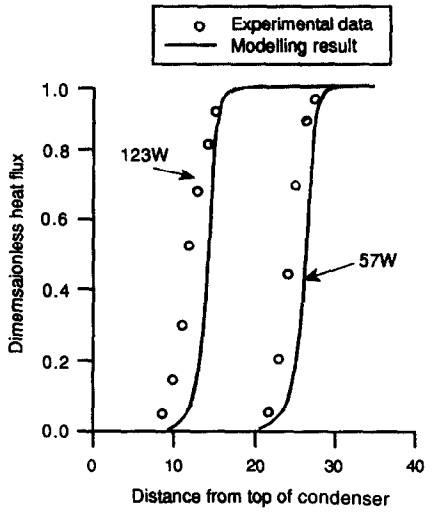

Fig. 7. Comparison of experimental and modelling results for a glass condenser at relatively high power levels with water as working fluid and air as non-condensable gas. The data points show the experimental values of dimensionless heat flux (equivalent to dimensionless temperature in this case). The lines are the results of the modelling calculations.

condenser; (b) the dimensionless temperature at the inner surface of the condenser (which is essentially the same as the dimensionless heat flux in this case); (c) the values of gas mole fraction in the volume of the condenser; and (d) gas mole fraction at the inner surface of the condenser. The values of gas mole fraction corresponding to each line in Fig. 8(c) can be obtained by extrapolating the lines to the condenser wall and reading the corresponding value in Fig. 8(d).

In Fig. 8(b), we also show experimental measurements of the dimensionless temperature (or heat flux) in the glass condenser. As can be seen, the agreement between experimental and numerical results is very good, providing strong evidence that, at these low power levels, convective effects are small.

The diffusion model predicts that the width of the interface will decrease as the power level increases, with a corresponding increase in the temperature difference across the interface $T_s - T_c$, in equation (19). This effect should be observable experimentally. However, measurements of the width of the interface in the glass condenser at slightly higher power levels than in Fig. 8 give an essentially identical result. We believe that the decrease in the width of the interface predicted by the diffusion model is effectively balanced by a small increase associated with convective effects at higher power levels. It was not possible to obtain good data for a glass condenser at lower power levels than those shown in Fig. 8, as these data represent the limit of resolution of the experiment.

Figure 9 shows experimental and numerical data for a copper condenser at two power levels (30 and 40 W) corresponding to low heat flux densities below the interface. The points in Fig. 9(a) show the measured thickness of the condensed liquid film, and the lines in this figure are numerical results from the diffusion model. The experimental results of film thickness are used to calculate the spatial dependence of heat flux, shown in dimensionless form in Fig. 9(b). Finally, Fig. 9(c) shows the dimensionless temperature difference between the condensing vapour and the cooling fluid obtained from the data of Fig. 9(b). Figure 9(c) also shows results from the diffusion model. However, the experimental and modelling results are in such good

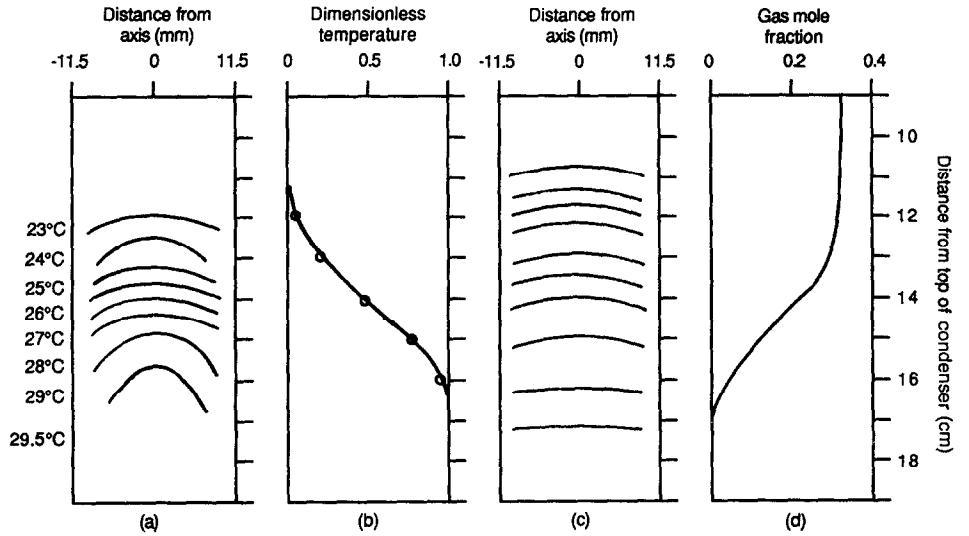

Fig. 8. Comparison of results from the diffusion model with experimental data at low power levels (84 W) in a glass condenser with water as working fluid and air as non-condensable gas. This figure shows: (a) calculated values of isotherms in the vicinity of the interface; (b) calculated (lines) and measured (points) dimensionless temperature (or dimensionless heat flux); (c) calculated surfaces of constant gas mole fraction; and (d) calculated values of gas mole fraction at the inner surface of the condenser. The values of gas mole fraction in (c) can be determined by projecting the curves to the wall of the condenser and reading off the corresponding value from (c). The experimental and modelling data in (b) are in very good agreement.

agreement that they are indistinguishable in these graphs.

The data of Fig. 9 also show that the experimentally measured width of the interface region for the lower power level (30 W) is very slightly greater than that at higher power (40 W), as predicted by the diffusion model. These results provide convincing evidence that, at these low power levels and for the small temperature differences that exist in the copper condenser, convective heat transfer in the interface region is negligible, and the condensation process is effectively influenced by diffusion only. It is clear from all of the results presented here, however, that in general this is not the case, and that convective effects usually play a large, and often dominant role in determining the nature of the heat and mass transfer in the vicinity of the interface of a gas-loaded thermosyphon.

6. CONCLUSION

The aim of this work was to identify the physical processes which determine the nature of the heat and mass transfer in the vicinity of the interface in a gas-loaded thermosyphon. Accurate measurements were made of the spatial dependence of condensing heat flux and temperature in condensers with highly conducting (copper) walls, and with relatively insulating (glass) walls.

Instabilities are observed in the vicinity of the interface at high power levels for a glass condenser, which are not associated with fluctuations in the vapour source. It is believed that these instabilities are triggered by small local variations in the condensing heat flux near the interface and that their existence indicates that the gas–vapour interface front is only marginally stable in an axially symmetric system. A small angular misalignment of the axis of the condenser with respect to the lower adiabatic region eliminates the fluctuations, and results in an interface region which does not possess cylindrical symmetry.

A numerical model was developed in which the transport processes in the interface region are determined by mass diffusion. The boundary conditions of the model are applied in a region well below the interface, and do not influence the calculated shape of the interface. A self-consistent method is used to solve the equations in cases where the condensation process is significantly influenced by the thickness of the condensed liquid film.

Experimental measurements of the width of the interface are in extremely good agreement with the diffusion model at low power levels, particularly for a copper condenser. For most power levels of practical importance, however, the width of the interface region is significantly greater than that predicted by the diffusion model, indicating the existence of an additional transport mechanism. The results obtained are consistent with the existence of significant heat and mass transport by convection at all but the lowest power levels.

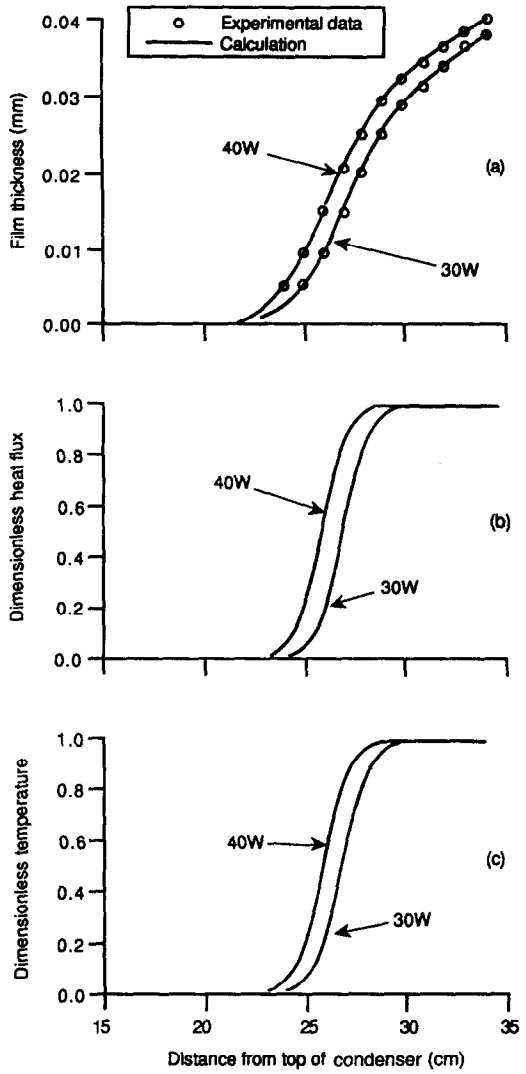

Fig. 9. Experimental and modelling results for a copper condenser at two different low levels of condensing heat flux below the interface. The working fluid is water, and air is the non-condensable gas. (a) Data for film thickness obtained experimentally (points) and from the diffusion model (lines). (b) The spatial dependence of condensing heat flux in the vicinity of the interface, obtained from the experimental results of (a). In (c), each line represents experimental and modelling data for the dimensionless temperature just inside the condenser wall. The experimental data are obtained from the heat flux results in (b). The experimental and modelling data at each power level in (c) are essentially identical.

Acknowledgments—This work was supported by His Royal Highness Prince Nawaf bin Abdul Aziz of the Kingdom of Saudi Arabia through the Science Foundation for Physics within the University of Sydney.

REFERENCES

1. B. D. Marcus, Theory and design of variable conductance heat pipes, N.A.S.A. Report CR-2018 (1972).
2. S. W. Chi, *Heat Pipe Theory and Practice*, pp. 124–155. Hemisphere, Washington, DC (1976).
3. D. K. Edwards and B. D. Marcus, Heat and mass transfer in the vicinity of the vapor-gas front in a gas-loaded heat pipe, *J. Heat Transfer* **94,** 155–162 (1972).
4. A. R. Rohani and C. L. Tien, Steady two-dimensional heat and mass transfer in the vapor–gas region of a gas-loaded heat pipe, *J. Heat Transfer* **95,** 377–382 (1973).
5. C. L. Tien and S. J. Chen, Non-condensable gases in heat pipes, *Proceedings of 5th International Heat Pipe Conference*, Japan, pp. 97–101 (1984).
6. K. Hijikata, S. J. Chen and C. L. Tien, Non-condensable gas effect on condensation in a two-phase closed thermosyphon, *Int. J. Heat Mass Transfer* **27,** 1319–1325 (1984).
7. A. A. Parfentleva and V. D. Portnov, Vapor flow in the condenser of a gas-regulated heat pipe, *J. Engng Phys.* **47,** 1061–1065 (1984).
8. V. V. Galaktionov and L. P. Trukhanova, Study of the process of heat and mass transfer in the region of the vapor–gas front in a gas-regulable heat pipe, *J. Engng Phys.* **48,** 296–300 (1985).
9. Y. Kobayashi and T. Matsumoto, Vapor condensation in the presence of non-condensable gas in the gravity assisted thermosyphon, *Proceedings of the 6th International Heat Pipe Conference*, France, pp. 565–570 (1987).
10. M. D. Parfentiyev, Heat transfer in the heat pipe condensation zone in the presence of a non-condensable gas, *Heat Transfer Sov. Res.* **19,** 95–102 (1987).
11. P. F. Peterson and C. L. Tien, Gas concentration measurements and analysis for gas-loaded thermosyphons, *A.S.M.E. Winter Annual Meeting* (1987).
12. Y. Kobayashi and T. Matsumoto, Two-dimensional condensing vapor flow on parallel flat plates in an enclosure, *J. Thermophys. Heat Transfer* **1,** 122–128 (1987).
13. X. Zhou and R. E. Collins, Condensation heat transfer in gas-loaded heat pipes, *Proceedings of the Fourth Australasian Conference on Heat and Mass Transfer*, Christchurch, New Zealand, pp. 441–448 (1989).
14. X. Zhou and R. E. Collins, Measurement of condensation heat transfer in a thermosyphon, *Int. J. Heat Mass Transfer* **34,** 369–376 (1991).
15. X. Zhou, Condensation heat transfer in a thermosyphon, Ph.D. thesis, University of Sydney (1991).
16. J. G. Reed and C. L. Tien, Modelling of the two-phase closed thermosyphon, *J. Heat Transfer* **109,** 722–730 (1987).
17. R. C. Reid, J. M. Prausnitz and T. K. Sherwood, *The Properties of Gases and Liquids* (3rd Edn), p. 548. McGraw-Hill, New York (1977).
18. E. R. Eckert and R. M. Drake Jr, *Heat and Mass Transfer* (2nd Edn), Appendix A9. McGraw-Hill, New York (1959).
19. A. M. Binnie, Experiments on the onset of wave formation on a film of water flow down a vertical plane, *J. Fluid Mech.* **2,** 551–553 (1957).
20. W. Nusselt, Die oberflaschenkondensation des wasserdampfs, *Z. Ver. Dt. Ing.* **60,** 541–569 (1916).